Visible-light photocatalytic activity of TiO_xN_y thin films obtained by reactive multi-pulse High Power Impulse Magnetron Sputtering

Alexandra Demeter, Florentina Samoila, Vasile Tiron, Dana Stanescu, Helene Magnan, Mihai Straticiuc, Ion Burducea, Lucel Sirghi

Surface & Coatings Technology xxx (2016) xxx–xxx

Contents lists available at ScienceDirect

Surface & Coatings Technology

journal homepage: www.elsevier.com/locate/surfcoat

Visible-light photocatalytic activity of TiO_xN_y thin films obtained by reactive multi-pulse High Power Impulse Magnetron Sputtering

Alexandra Demeter [a], Florentina Samoila [a], Vasile Tiron [a], Dana Stanescu [b], Helene Magnan [b], Mihai Straticiuc [c], Ion Burducea [c], Lucel Sirghi [a,*]

[a] Iasi Plasma Advanced Research Center (IPARC), Faculty of Physics, "Alexandru Ioan Cuza" University, Iasi 700506, Romania
[b] SPEC, CEA, CNRS, Université Paris-Saclay, CEA-Saclay, 91191 Gif-sur-Yvette Cedex, France
[c] Horia Hulubei National Institute of Physics and Nuclear Engineering, Magurele 077125, Romania

ARTICLE INFO

Article history:
Received 31 May 2016
Revised 30 September 2016
Accepted in revised form 3 October 2016
Available online xxxx

Keywords:
Titanium oxynitride
m-HiPIMS deposition
Visible-light photocatalyst
Water splitting

ABSTRACT

Reactive High Power Impulse Magnetron Sputtering operated in multi-pulse mode (m-HiPIMS) of a pure Ti target in $Ar/N_2/O_2$ gas mixture (mass flow rates of 50, 2 and 0.16 sccm, respectively) has been used for the deposition of titanium oxynitride (TiO_xN_y) thin films with variable content of nitrogen (from 0.6 at.% to 24.2 at.%). Increase of the nitrogen content in the deposited TiO_xN_y thin films determined a decrease of the optical bandgap energy and a corresponding increase of visible light adsorption. The photocatalytic activity for water molecule splitting of the films deposited on metallic substrate, which were used as the photo-anode in an electrochemical cell, has been investigated by measurements of photoelectrochemical current intensity versus biasing voltage during on/off cycles of visible light irradiation (sun light simulated by a xenon lamp). The as-deposited films have a short range order corresponding to rutile and anatase structures and showed very weak photocatalytic activity and chemical instability in the electrolyte of the photoelectrochemical cell. However, a post-deposition annealing treatment of the film with low content of nitrogen (0.6 at.%) improved considerably the visible-light photocatalytic activity, the film crystalline order and chemical stability.

1. Introduction

Since the discovery of photocatalytic water splitting by Honda and Fujishima [1], titanium dioxide has been intensively studied as an environmental material with applications in photocatalytic purification of air and water and hydrogen fuel production from photocatalytic splitting of water molecules [2]. Among other photocatalyst semiconductors, TiO_2 has been the most investigated material because, on one hand, it is regarded as a theoretical material model of photocatalyst semiconductors [3] and, on the other hand, it has very attractive properties for photocatalysis applications as low cost, high chemical stability, long lifetime of electron/hole pairs and high oxidizing power of photogenerated holes [4]. However, the large bandgap of TiO_2 (3.2 eV for anatase and 3 eV for rutile) [5] restricts its good photocatalytic activity to a small fraction of solar energy radiation (UV light). Therefore, a large number of studies have been dedicated to extension of the photocatalytic activity of TiO_2 to visible light. A good photocatalyst semiconductor for water splitting under solar light should have the minimum energy of the conduction band (CBM) higher than the potential energy for hydrogen reduction (H^+/H_2) and the maximum of the valence band (VBM) lower than the potential energy of oxygen oxidation (O^-/O_2), which is at −1.23 eV (versus the NHE). For anatase TiO_2 the CBM is just above the H^+/H_2 reduction energy level (0.37 eV), while the VBM is located deeply at −2.83 eV (versus NHE) [6]. Therefore, visible light photocatalysts developed from the TiO_2 structure used doping with metal cations or acceptor anions for engineering the band energy structure of this material. Compared to cation doping, the anions doping is less likely to form charge recombination sites and is, therefore, considered a more effective approach used for enhancing the photocatalytic activity of TiO_2. However, Yan et al. [6] have found that TiO_2 co-doping with Zr cations and N anions is more effective than doping with either cations or anions. Asahi et al. [7] have theoretically evaluated the effect on the band energy structure of substitutional doping with C, N, F, P and S anions for O in anatase TiO_2 and found N as the best candidate for engineering the TiO_2 energy band structure for visible light photocatalyst applications. In N-doped TiO_2, the p states of N mix with 2p of O, thus shifting the VBM upwards without notably changing the position of CBM. Since the pioneering work of Asahi et al. [7], many authors tried to synthesize good photocatalyst semiconductors based on nitrogen doped titanium dioxide or titanium oxynitride (TiO_xN_y) [8]. However, the fact that the states introduced by dopant atoms act as recombination centers for electron–hole pairs as well as the thermal instability associated with doped materials humpered the photocatalytic performance of

* Corresponding author.
E-mail address: lsirghi@uaic.ro (L. Sirghi).

http://dx.doi.org/10.1016/j.surfcoat.2016.10.011
0257-8972/

these new materials. The photo-catalytic process is also strongly affected by bulk material properties, such as crystallinity, a better crystallinity increasing the life time and mobility of charge carriers [9]. In general, the photocatalytic semiconductors with high defect density have a weak photocatalytic activity because of the formation of charge recombination centers. Recently, Yabi et al. [10] have predicted the $Ti_3O_3N_2$ crystal as a new water-splitting photocatalytic material. The predicted value for instability energy, $\Delta H = 31$ MeV/atom, indicates that this material can be synthesized. However, synthesis of this material has been not reported so far. The predicted band edge structure of $Ti_3O_3N_2$ is interesting for visible light water-splitting photocatalysis because the CBM and VBM bracket the water redox levels and the energy bandgap is 2.37 eV. Due to this low value of the energy bandgap, the $Ti_3O_3N_2$ crystal may exhibit better photocatalytic performance than TaON, the best known oxynitride photocatalyst so far [11].

In this work, we investigate the capability of the reactive High Power Impulse Magnetron Sputtering (HiPIMS) deposition technique to synthesize TiO_xN_y thin films with good visible light photocatalytic activity for water splitting. This deposition technique showed good reproducibility and process stability for synthesis of oxides, nitrides or oxynitrides thin films [12], which otherwise are difficult to achieve by more conventional magnetron sputtering techniques [13,14]. In a previous work [15], we have shown that reactive HiPIMS [16] working in multi-pulse mode (m-HiPIMS) [17] in Ar/O_2 gas mixture (0.2% O_2 of the total mass flow rate) can be easily manipulated for synthesis of substoichiometric TiO_x thin films with x values down to 1.63. The deficit of oxygen in the deposited TiO_x films was controlled by the HiPIMS pulse repetition frequency. Increase of this parameter determined a transition from oxidized towards metallic target sputtering with a noticeable increase of the sputtered Ti atoms in the gas phase. The limited amount of oxygen in the deposition chamber and the increased amount of sputtered Ti determined depositions of TiO_x thin films with a large deficit of oxygen at large values of the HiPIMS pulsing repetition rate. By adding nitrogen to the working gas, the excess of sputtered metal atoms and limited amount of oxygen content favour depositions of metal oxynitride films with larger content of nitrogen. Recently, we have proved this mechanism in the case of ZnO_xN_y thin films. Here, we use reactive m-HiPIMS depositions in $Ar/O_2/N_2$ gas mixture for synthesis of TiO_xN_y with the content of N ranging from 0.6 at.% to 24.2 at.% (which is close to the N concentration in the predicted $Ti_3O_3N_2$ material). Structure and composition of deposited films have been investigated by atomic force microscopy (AFM), X-ray diffraction (XRD), Rutherford Backscattering Spectroscopy (RBS), Raman spectroscopy and X-ray photoelectron spectroscopy (XPS). The adsorption and photogeneration of electron–hole pairs under visible light irradiation were investigated by optical transmission spectroscopy measurements. The photocatalytic activity for water splitting under visible light illumination has been investigated by measurements of photoelectrochemical current intensity variations versus biasing voltage during on/off cycles of visible light irradiation (sun light simulated by a xenon lamp).

2. Experimental devices, methods and techniques

In the m-HiPIMS, a single voltage pulse applied to the cathode (−700 V in peak value) with 15 μs in width was decomposed into a sequence of 3 individual micropulses with the width of 5 μs. By doing this, the sputtering rate has been noticeably improved due to diminished back attraction of sputtered and ionized atoms. The delay time between the micropulses within a sequence was kept constant (50 μs) in all the experiments. The value of 50 μs for the delay time between micropulses in m-HiPIMS has been chosen to optimize the m-HiPIMS deposition [17]. Typical time variations of the current intensity and discharge voltage during m-HiPIMS operation at sequence repetition frequency values of 400 and 1600 Hz are given in Fig. 1. Apart of a decrease of preionization voltage from −310 V to −20 V, the voltage waveform does not change noticeably with the increase of the sequence repetition

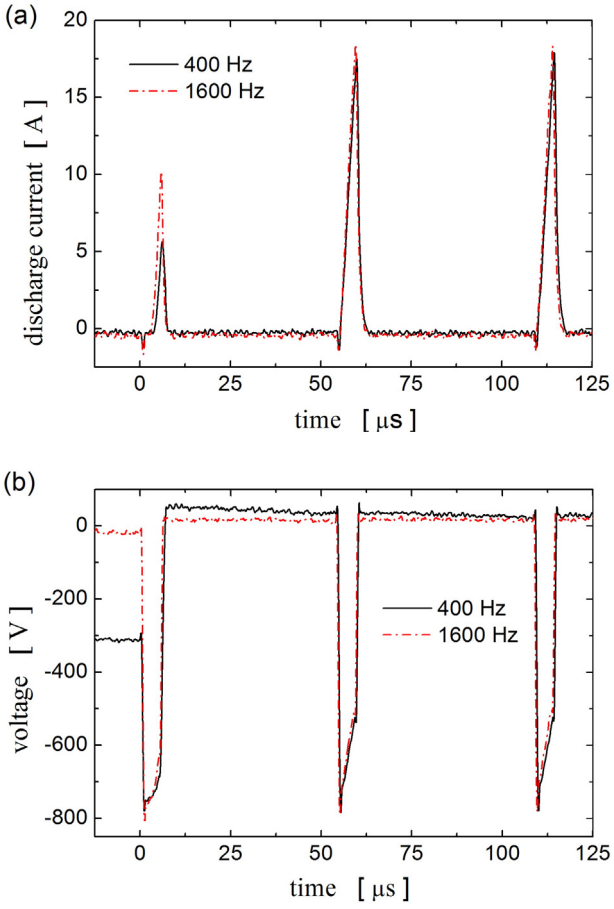

Fig. 1. Typical waveforms of the current intensity (a) and discharge voltage (b) for m-HiPIMS (sequence of three micropulses of 5 μs in width separated by time-off periods of 50 μs) at sequence repetition frequency values of 400 and 1600 Hz, respectively.

frequency from 400 Hz to 1600 Hz. The role of the pre-ionization is to provide between discharge pulses certain ionization degree of the working gas (very weak plasma), which prevents giant impedance jumps when switching from insulator to conductor (plasma) gas state. It is worth mentioning that, at high sequence repetition frequency the pre-ionization is no longer required, its role being played by the residual charged species surviving in the afterglow plasma. The peak value of the current intensity corresponding to the first micropulse from the multipulse sequence is sensitive to the repetition frequency due to a change of target surface condition during the long time between consecutive micropulse sequences. At low repetition frequency the discharge operates in compound mode, the target surface being covered with oxynitride compound, which determines a lower value of the peak discharge current intensity for the first micropulse. As the repetition frequency increase, the period between sequences becomes smaller and the target surface becomes less poisoned. The average power increases linearly from 20 to 80 W as the sequence repetition frequency increases from 400 to 1600 Hz. By increasing the m-HiPIMS pulsing repetition frequency, the amount of sputtered Ti increases and, due to the limited amount of oxygen in the deposition chamber, depositions of films with larger content of nitrogen is favoured.

All the experiments were performed in a high vacuum stainless steel chamber using a Ti target (99.995% purity, produced by Kurt J. Lesker Company) with a diameter of 50 mm and thickness of 5 mm. A low content in oxygen of the working gas was chosen to facilitate incorporation of nitrogen in the deposited TiO_xN_y thin films. Thus, the working gas was a mixture of Ar (mass flow rate of 50 sccm) and O_2 (mass flow rate of 0.16 sccm) and N_2 (mass flow rate of 2 sccm) at the total pressure

Please cite this article as: A. Demeter, et al., Surf. Coat. Technol. (2016), http://dx.doi.org/10.1016/j.surfcoat.2016.10.011

of 0.85 Pa. Use of a larger concentration of oxygen in the working gas determined depositions of pure TiO_x thin films (negligible content of nitrogen) regardless the HiPIMS pulse repetition frequency. Incorporation of nitrogen in the as-deposited films was facilitated also by the use of room temperature for the deposition substrates. Increase of the substrate temperature determined a drastic decrease of nitrogen content of the deposited films. The TiO_xN_y thin films were deposited on quartz, glass and copper substrates placed at on the target axis at a distance of 50 mm from the target. The deposition rate was measured by a quartz crystal microbalance (QCM) placed beside the substrate. The thickness of the deposited films was monitored by the QCM and kept around 100 nm by adjusting the deposition time. Details on the set-up and m-HiPIMS technique have been given in a previous work [17].

The crystalline structure of the deposited thin films was investigated by an X-ray diffractometry and Raman spectrometry. The X-ray diffractometer (LabX XRD-6000 from Shimadzu Co.) used Cu-Kα X-ray source ($\lambda = 1.54059$ A) in Bragg–Brentano configuration. The films were analyzed in the range of $2\theta = 10°–50°$, with a scanning rate of 4°/min and a grazing incidence angle of 2°. The Raman spectrometer (LabRAM HR-800, Horiba-Jobin Yvon) was used in the back-scattering configuration to collect spectra at room temperature in the range 100–1000 cm^{-1} of the films excited by a 632 nm Ar^+ laser line excitation. The scattered light was detected by a water-cooled charge coupled device detector.

The chemical composition of the deposited films was investigated by X-ray Photoelectron Spectroscopy (PHI 5000 VersaProbe XPS system from ULVAC PHI, Inc.) and Rutherford Backscattering Spectrometry (RBS) measurements. The RBS used a monochromatic (3.72 MeV) $^4He^{2+}$ ions beam and non-Rutherford ^{14}N (^4He, ^4He) ^{14}N scattering cross-section resonance at 3.72 MeV for TiO_xN_y sample analysis. The measurements were performed in IBM geometry with an incident angle of 7°, in order to avoid channeling effects, and a laboratory scattering angle of 165°. Scattered particles were registered with an AMETEK type BU-012-050-100 charged particle detector, having a solid angular acceptance of 1.641 msr and connected to a standard spectrometric chain and acquisition system. The typical energy resolution of the spectrometer was 18 keV. The RBS spectra were evaluated using SIMNRA code.

The topography images and roughness of the deposited film surfaces have been obtained by atomic force microscopy (AFM) measurements performed in non-contact mode with a silicon AFM probe (NSG 03 from NT-MDT, Russia) with a sharpened tip (nominal curvature radius of 10 nm) and a stiff cantilever (resonant frequency of 150 kHz and force constant of 6.1 N/m).

The optical band-gap of the deposited films on quartz substrates were estimated from optical transmittance spectra obtained by a UV–VIS spectrophotometer. The photocatalytic activity of the deposited TiO_xN_y thin films was characterized by photo-electrochemical (PEC) response and methylene blue (MB) degradation measurements. The PEC response, light excitation efficiency and photo-sensitivity of TiO_xN_y films deposited on copper substrates were tested in a conventional three electrode arrangement electrochemical cell with aqueous electrolyte solution (0.1 M NaOH). The films loaded on the PEC cell were irradiated by an ozone-free Xe arc lamp mimicking the AM 1.5 solar spectrum at midday for mid-latitudes (100 mW/cm^2 in wavelength range 200–1000 nm). The infrared radiation was filtered just after the lamp output to avoid inconvenient heating of the experimental setup. Details on the experimental procedures and equipment for the PEC measurements have been described in [18]. For the MB decomposition experiments, the films deposited on quartz (1×1 cm^2 in size) were immersed in aqueous MB solution (6 ml) and then irradiated by visible light ($\lambda > 400$ nm, incident light flux 120 mW/cm^2 homogeneously distributed over a surface area of 1.6 cm^2) for a total time of 2 h. The concentration of MB solution was determined after every 5 min of irradiation by measurements with a UV–VIS spectrophotometer of the absorbance peak at wavelength 664 nm. The same quantity of MB solution without any immersed film has been used as control.

3. Results and discussion

In this work, six TiO_xN_y thin films (samples labeled from S1 to S6) were successively deposited by m-HiPIMS at different values of pulse sequence repetition frequency on glass, quartz and copper substrates at room temperature. In Table 1 are presented atomic composition, optical bandgap values, and the visual aspect (color) of the six samples. The following subsections present the results concerning investigations of film structure and composition, and their optical and photocatalytic properties.

3.1. Structure, composition and optical bandgap

The atomic composition of the TiO_xN_y thin films deposited on glass substrates was determined by means of Rutherford Backscattering Spectroscopy (RBS). The results for six samples (S1 to S6) obtained by HiPIMS depositions at six values of pulse sequence repetition frequency are presented in Table 1. The increase of the m-HiPIMS repetition frequency from 750 to 1600 Hz determined an increase of the N content of the deposited TiO_xN_y thin films from 0.6 at.% to about 24 at.%. The value of N content in the film deposited at m-HiPIMS pulse repetition frequency of 1600 Hz is close to the N content in the stoichiometric $Ti_3O_3N_2$ compound (25 at.%). The mechanism explaining the effect of m-HiPIMS repetition frequency on the nitrogen content of the deposited films is based on the fact that the sputtered titanium atoms are more reactive towards oxygen than towards nitrogen. The oxygen content of the working gas was set to a very low value (0.16%) to determine a deficit of oxygen in the deposited films [15]. By increasing of m-HiPIMS repetition frequency, the amount of sputtered titanium atoms is increased, which means that a larger amount of titanium is available for reactions with nitrogen, after all the oxygen atoms from the deposition chamber were consumed.

The optical properties of the films were determined from their transmittance spectra recorded using an UV–VIS spectrophotometer. Optical transmittance spectra recorded in the wavelength range 300–1100 nm are shown in Fig. 2. It is noticed that the optical absorption edge is shifted towards longer wavelengths with the increased content of nitrogen in the as-deposited films, which at its turn increased with the increase of HiPIMS pulse sequence repetition frequency. The energy bandgap of the TiO_xN_y films was calculated from the linear fit of the linear portion from the $(\alpha h\nu)^{1/2}$ vs. $h\nu$ plot at the optical absorption edge. The obtained results indicate that the energy band-gap (E_g) gradually decreases from 3.18 eV (for the films with 0.6 at.% content of N) to 1.09 eV (for the films with 24.2 at.% content of N). Fig. 3 presents the dependencies of nitrogen content and energy bandgap on the m-HiPIMS

Table 1
Atomic content and energy bandgap of six TiO_xN_y thin films deposited at various values of m-HiPIMS pulse repetition frequency.

Sample	S1	S2	S3	S4	S5	S6
Frequency (Hz)	750	1000	1150	1250	1400	1600
N (at.%)	0.6	12	15.6	17.2	22	24.2
O (at.%)	63.2	55.4	51.5	49.8	43.8	40.17
Ti (at.%)	36.2	32.6	32.8	33	34.2	35.6
Bandgap (eV)	3.18	2.35	1.72	1.65	1.15	1.09
Color (on copper)	Yellow	Pink	Green	Dark green	Dark blue	Dark blue

Please cite this article as: A. Demeter, et al., Surf. Coat. Technol. (2016), http://dx.doi.org/10.1016/j.surfcoat.2016.10.011

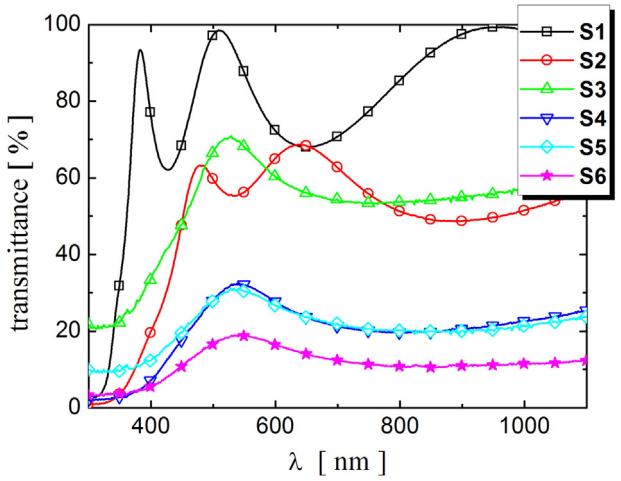

Fig. 2. UV–VIS transmission spectra of TiO_xN_y thin films deposited on quartz substrates.

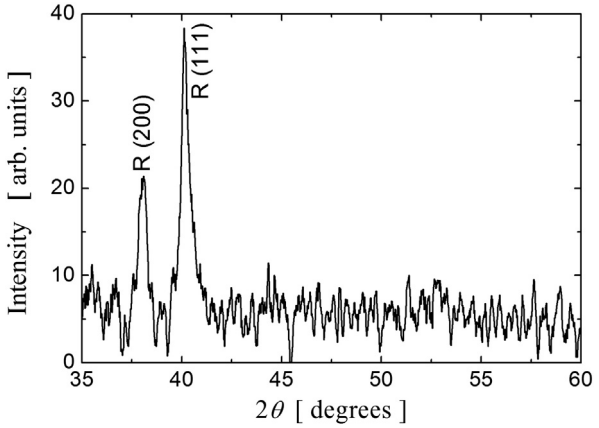

Fig. 4. The XRD pattern of sample S1 after annealing. The peaks at 38 and 40° are attributed to formation of rutile nanocrystalites in the film structure [19].

pulse sequence repetition frequency values. The values of energy bandgap of the six TiO_xN_y films are also presented in Table 1.

The crystalline structure of the as-deposited and thermal annealed films was investigated by X-ray diffraction and Raman spectroscopy measurements. The X-ray diffraction patterns acquired at grazing incidence for the as-deposited films showed no diffraction peaks. Incorporation of right amount of nitrogen and annealing treatment at high temperature might lead to formation of oxynitride crystalline phases. Therefore, we annealed the deposited films for one hour in nitrogen atmosphere at 400 °C. However, only the sample S1 showed presence of diffraction peaks, which correspond to rutile (1 1 1) and (2 0 0) TiO_2 phase (Fig. 4). The annealing treatment did not have the same effect for the films with larger content of nitrogen, which remained amorphous (with short range order structures). We believe that formation of crystalline phases in the films with high content of nitrogen is hampered by the large number of interstitial nitrogen atoms.

The structure of TiO_xN_y thin films was investigated also by Raman spectroscopy. The Raman spectra of the as-deposited samples confirmed that the samples present almost amorphous structures, The Raman spectra of the samples after thermal annealing (shown in Fig. 5) confirmed the results of the XRD investigation. Intense Raman peaks appear only for the sample with small amount of nitrogen (S1), indicating a high degree of crystallinity. The typical Raman modes at 145, 396, 445, 496, 613 and 640 cm^{-1} are assigned to the E_g(A), B_{1g}(A), E_g(R), B_{1g}(A), A_{1g}(R), and E_g(A) modes in anatase and rutile structures [20]. The strongest modes at 145, 613 and 640 cm^{-1} indicate that anatase and rutile phases with a long-range order have been obtained only for the sample S1.

The X-ray photoelectron spectroscopy measurements have been done to investigate the chemical composition and bonding of nitrogen in the annealed TiO_xN_y films. The stoichiometry of the deposited films has been evaluated from integrated peak areas of Ti-2p, O-1s and N-1s XPS signals with appropriate correction factors. The results confirmed the atomic composition of the films found by the RBS investigation (Table 1). Fig. 6 shows the structure of Ti 2p core electron levels in the annealed film S2 containing around 12 at.% nitrogen. The Ti-2p signal has been resolved into four contributions: two peaks at 458.5 eV and 464.2 eV attributed to Ti^{4+}—O_2^{2-} bonds and two peaks at 456.3 eV and 462.3 eV assigned to Ti^{+3}—N^{3-} bonds [21]. Unfortunately, it is hard to discriminate between titanium nitride and titanium metallic signals due to closeness of the corresponding electronic states [15,22]. The N-1s signal (not shown) has shown a strong peak at 396.4 eV corresponding to N—Ti bonds and a weak peak at 399.8 eV corresponding to adsorbed N_2 [23]. In conclusion, the XPS measurements indicate that most of nitrogen is chemically bounded to titanium atoms with possible excess of titanium atoms.

The atomic force microscopy measurements revealed no noticeable differences in surface morphology of the either as-deposited or annealed thin films, the root mean square roughness having values

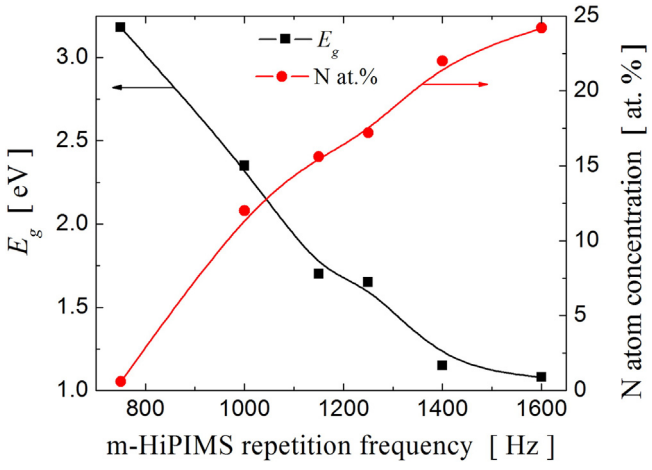

Fig. 3. Content of N and energy bandgap of TiO_xN_y thin films deposited at various values of HiPIMS pulse sequence repetition frequency.

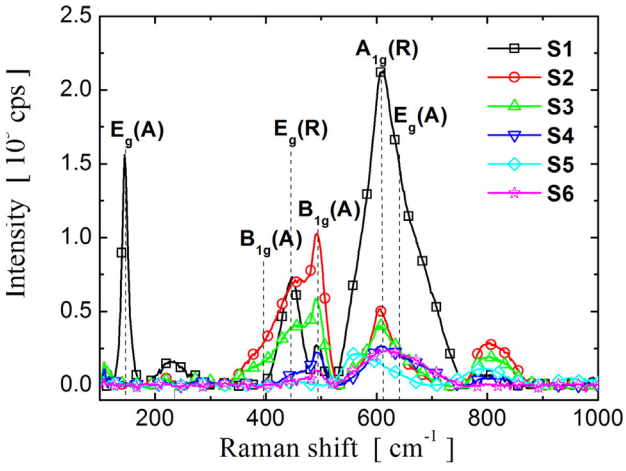

Fig. 5. Raman spectra of TiO_xN_y thin films deposited by m-HiPIMS at various values of repetition frequency. The micro-Raman spectra have been collected at room temperature with a Raman spectrometer operating with the 632 nm spectral line in backscattering geometry in the range of 100–1000 cm^{-1}.

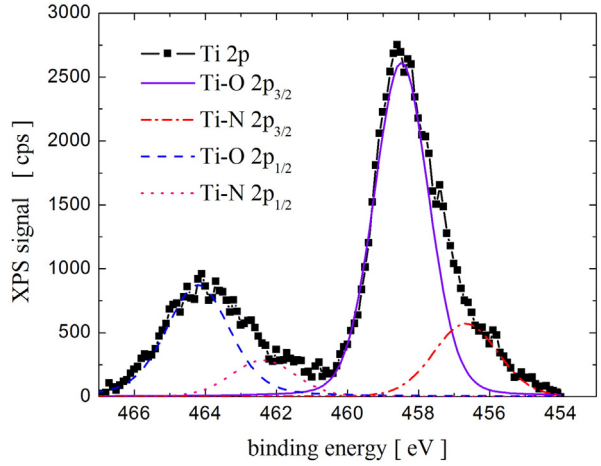

Fig. 6. The XPS signal corresponding to Ti 2p states in the film S2 (12 at.% nitrogen). The base line has been extracted from the XPS signal.

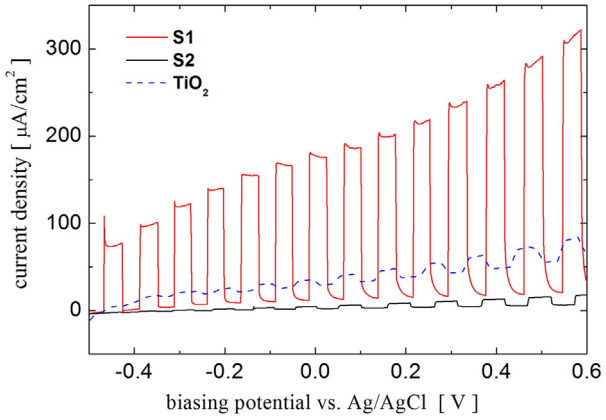

Fig. 8. Chopped light polarization curves of the annealed TiO_xN_y thin films S1 (0.6 at.% nitrogen), S2 (12 at.% nitrogen) and a TiO_2 thin film deposited by m-HiPIMS in the same experimental conditions as S1, excepting the composition of the working gas, which did not contain oxygen. The incident UV light flux of 100 mW/cm^2, electrolyte 0.1 M NaOH, scan rate of 50 mV s^{-1}.

around 0.5 nm have been found for all the investigated TiO_xN_y film surfaces.

3.2. Photocatalytic activity

The visible-light photocatalytic activity of the as-deposited TiO_xN_y thin films has been estimated firstly by measurements of the efficiency of the films irradiated by visible light ($\lambda > 400$ nm) for photocatalytic degradation of methylene blue (MB) molecules in an aqueous solution. For all the as-deposited films, the photocatalytic activity for MB molecule degradation was weak. Then, the TiO_xN_y films were annealed for one hour in nitrogen atmosphere at 400 °C in order to improve the film crystalline order and enhance their photocatalytic activity. The annealing treatment resulted in a noticeable improvement of photocatalytic activity only for the film with the smallest content of nitrogen (S1). Fig. 7 is showing comparatively the time evolution of MB concentration as result of photocatalytic degradation of MB on the visible-light irradiated film S1 before and after annealing treatment. As resulted from the X-ray diffraction investigation of the annealed sample S1, this improvement of photocatalytic activity can be attributed to the improvement of the crystalline order in the film. Indeed, the X-ray diffraction pattern of the sample S1 after annealing treatment shows presence of rutile (1 1 1) and rutile (2 0 0) diffraction peaks (Fig. 4). Incorporation of right amount of nitrogen and annealing treatment at higher temperature might lead to formation of oxynitride crystalline phases.

The photocatalytic activity for water molecule splitting of the annealed TiO_xN_y films deposited on copper substrates used as photoanodes in a photoelectrochemical (PEC) cell has been evaluated. The PEC response of the as-deposited and annealed films with large content of nitrogen was extremely weak. Moreover the as-deposited films were not stable during PEC measurements, they being etched by the NaOH solution. Compared to the annealed TiO_xN_y thin films with large content of nitrogen, the annealed film S1 (with 0.6 at.% of nitrogen) showed a much better photocatalytic activity in visible light. Fig. 8 shows the comparison between PEC response of the annealed films S1 and S2 illuminated by time-chopped light from a xenon lamp simulating the sunlight [18]. For the film S2 (12 at.% nitrogen), it has been observed a very small photocurrent (defined as the difference between dark and light current). The low photocatalytic activity of the films with high content of nitrogen could be caused by the high density of defects (e.g. oxygen vacancies). For the film S1, a maximum PC density of 0.3 mA/cm^2 was obtained for a bias of 0.6 V vs. Ag/AgCl, which shows the good photocatalytic activity for water splitting of this film. Also in Fig. 8, the PEC response for photocatalytic water splitting of the TiO_xN_y thin films S1

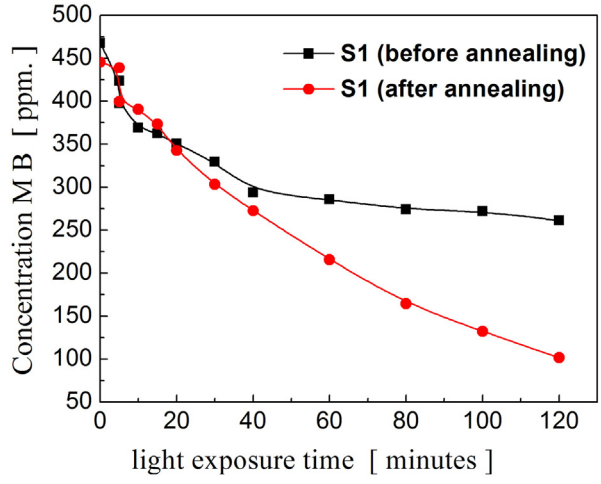

Fig. 7. Time variation of MB concentration in aqueous solution due to photocatalytic decomposition of MB under visible light radiation ($\lambda > 400$ nm, power density = 120 mW/cm^2) showing improvement of photocatalytic activity of sample S1 as result of post-deposition annealing treatment.

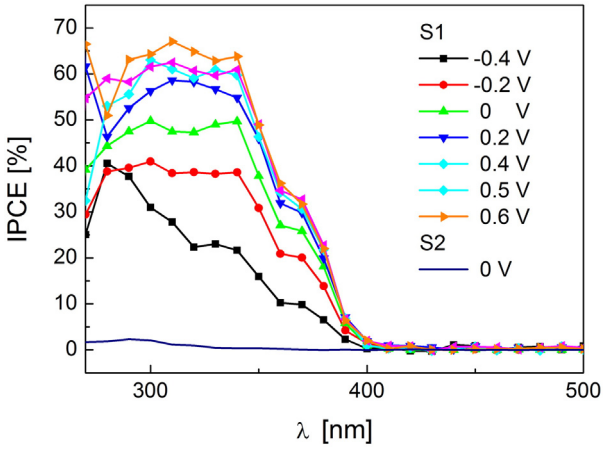

Fig. 9. Incident-Photon-to-Current-Efficiency (IPCE) measured at various values of biasing potential (vs. Ag/AgCl) for the annealed TiO_xN_y thin films S1 (0.6 at.% nitrogen).and S2 (12 at.% nitrogen).

and S2 is compared with the PEC response of a pure TiO_2 thin film (deposited by m-HiPIMS in the same experimental conditions as S1, excepting the composition of the working gas, which did not contain oxygen). The PEC response of the TiO_2 film was much weaker than the PEC response of S1, but larger than the PEC response of S2. This means that incorporation of small amount of nitrogen in TiO_2 thin films is beneficial for the film photocatalytic activity, while incorporation of larger amount of nitrogen is detrimental, probably due to the large number of defect states (low crystalline order) associated with incorporation of large amounts of nitrogen.

The wavelength dependence of the Incident-Photon-to-Current-Efficiency (IPCE) for the films S1 and S2 was measured at various values of biasing potential (vs. Ag/AgCl). The IPCE was calculated with [18]:

$$IPCE(\lambda) = \frac{h \cdot c}{\lambda} \cdot \frac{J_{ph}(\lambda)}{e \cdot P(\lambda)} (\%) \quad (1)$$

where $J_{ph}(\lambda)$ is the photocurrent density, $P(\lambda)$ the incident power density, λ the wavelength of the incident light, h the Planck constant (6.62×10^{-34} J.s), c the light velocity (3×10^8 m/s), and e the elementary charge (1.6×10^{-19} C). Fig. 9 shows the variation of IPCE versus wavelength for the samples S1 and S2. It is noticed that IPCE of the sample S2 was very low, irrespective of the wavelength value. For the sample S1, the IPCE values show very good quantum efficiency for UV radiation (about 60% at a biasing potential of 0.5 V) and a cutoff (fast drop of values) at 400 nm. This means that the incorporation of nitrogen in the film S1 resulted in a slight decrease of the bandgap of this film and, thus, improved slightly its photocatalytic activity in visible light. Therefore, its good PEC response in sun light (simulated by the xenon lamp) is owed mainly to the UV radiation.

4. Conclusion

We have investigated the capability of HiPIMS deposition technique to synthesize TiO_xN_y thin films with visible light photocatalytic activity for water splitting. To increase the deposition rate and probabilities of chemical reactions in the deposition chamber, we operate the HiPIMS discharge in multiple pulse mode (m-HiPIMS), i.e. a pulse with 15 μs in width was split in three micro-pulses with 5 μs in width. It has been shown that the concentration of N atoms in the m-HiPIMS deposited TiO_xN_y thin films can be controlled by pulse sequence repetition frequency provided the oxygen content in the working gas is low (mass flow ratio of 0.16 sccm for O_2, 2 sccm for N_2 and 50 sccm for Ar) and the substrates were kept at room temperature. Thin TiO_xN_y films with nitrogen content ranged between 0.6 at.% and 24 at.% were obtained by increasing the m-HiPIMS repetition frequency from 750 Hz to 1600 Hz. The as-deposited TiO_xN_y films had short-range order corresponding to anatase and rutile structures and showed weak photocatalytic activity. For the film with very low content of nitrogen, a post deposition annealing treatment resulted in a noticeable improvement of crystalline order and photocatalytic activity. The films with higher content of nitrogen showed no improvement in crystalline order or photocatalytic activity as result of the annealing treatment. When comparing the film activity for water splitting, a pure TiO_2 thin film showed much weaker activity than the TiO_xN_y film with low content of nitrogen (0.6 at.%) and higher activity than the TiO_xN_y films with higher content of nitrogen (>12 at.%). Therefore, we conclude that incorporation of small amount of nitrogen in TiO_2 thin films is beneficial, while incorporation of larger amount of nitrogen is detrimental for the film photocatalytic activity in visible light. These results point to the important role of crystalline order for improving of the photocatalytic activity of semiconductors in visible light, besides the role of a smaller energy bandgap. Although we did not obtain crystalline TiO_xN_y films in this work, we proved that the amount of nitrogen incorporated into the films deposited by m-HiPIMS can be easily controlled. Post deposition treatments as the thermal annealing in nitrogen might improve the film crystalline order and photocatalytic activity and this will be subject for further investigations.

Acknowledgements

This work was supported by Joint Research Projects PN-II-ID-JRP-2012-RO-FR-0161.

References

[1] A. Fujishima, K. Honda, Electrochemical photolysis of water at a semiconductor electrode, Nature 238 (1972) 37.
[2] K. Hashimoto, H. Irie, A. Fugishima, TiO_2 photocatalysis: a historical overview and prospective, Jpn. J. Appl. Phys., Part 1 44 (2005) 8269–8295.
[3] A.V. Emeline, A.V. Frolov, V.K. Ryabchuk, N. Serpone, Spectral dependencies of the quantum yield of photochemical processes on the surface of nano/micro-particulates of wide-band-gap metal oxides. IV. Theoretical modeling of the activity and selectivity of semiconductor photocatalysts with inclusion of a subsurface electric field in the space charge region, J. Phys. Chem. B 107 (2003) 7109–7119.
[4] A. Fujishima, X. Zhang, D.A. Trik, TiO_2 photocatalysis and related surface phenomena, Surf. Sci. Rep. 63 (2008) 515.
[5] K. Rajeshwar, Photoelectrochemistry and the environment, J. Appl. Electrochem. 25 (1995) 1067.
[6] H. Yan, X. Wang, M. Yao, X. Yao, Band structure design of semiconductors for enhanced photocatalytic activity, Prog. Nat. Sci.: Mater. Int. 23 (4) (2013) 402–407.
[7] R. Asahi, T. Morikawa, T. Ohwaki, K. Aoki, Y. Taga, Visible-light photocatalysis in nitrogen-doped titanium oxides, Science 293 (2001) 269–271.
[8] L.G. Devi, R. Kavitha, Review on modified N–TiO_2 for green energy applications under UV/visible light: selected results and reaction mechanisms, RSC Adv. 4 (2014) 28265–28299.
[9] A. Kudo, Photocatalysis and solar hydrogen production, Pure Appl. Chem. 79 (2007) 1917.
[10] Y. Wu, P. Lazic, G. Hautier, K. Persson, G. Ceder, First principles high throughput screening of oxynitrides for water-splitting photocatalysts, Energy Environ. Sci. 6 (1) (2012) 157.
[11] K. Maeda, K. Domen, Photocatalytic water splitting: recent progress and future challenges, J. Phys. Chem. Lett. 1 (2010) 2655.
[12] M. Aiempanakit, P. Larsson, K. Sarakinos, J. Jensen, T. Kubart, U. Helmersson, Hysteresis and process stability in reactive high power impulse magnetron sputtering of metal oxides, Thin Solid Films 519 (2011) 7779.
[13] M. Nicolas, J. Lintymer, J. Gavoille, J.-M. Chappé, F. Sthal, J. Takadoum, F. Vaz, L. Rebouta, Reactive sputtering of TiO_xN_y coatings by the reactive gas pulsing process: part III: the particular case of exponential pulses, Surf. Coat. Technol. 201 (2007) 7733–7738.
[14] M. Nicolas, J. Lintymer, J. Gavoille, J.-M. Chappé, F. Sthal, J. Takadoum, F. Vaz, L. Rebouta, Reactive sputtering of TiO_xN_y coatings by the reactive gas pulsing process: part II: the role of the duty cycle, Surf. Coat. Technol. 201 (2007) 7727–7732.
[15] V. Tiron, I.-L. Velicu, M. Dobromir, A. Demeter, F. Samoila, C. Ursu, L. Sirghi, Reactive multi-pulse HiPIMS deposition of oxygen-deficient TiO_x thin films, Thin Solid Films 603 (2016) 255–261.
[16] V. Kouznetsov, K. Macák, J.M. Schneider, U. Helmersson, I. Petrov, A novel pulsed magnetron sputter technique utilizing very high target power densities, Surf. Coat. Technol. 122 (1999) 290.
[17] O. Antonin, V. Tiron, C. Costin, G. Popa, T.M. Minea, On the HiPIMS benefits of multi-pulse operating mode, J. Phys. D. Appl. Phys. 48 (2015) 015202.
[18] M. Rioult, H. Magnan, D. Stanescu, A. Barbier, Single crystalline hematite films for solar water splitting: Ti-doping and thickness effects, J. Phys. Chem. C 118 (2014) 3007.
[19] J. Lynch, Cinzia Giannini, J.K. Cooper, A. Loiudice, I.D. Sharp, R. Buonsanti, Substitutional or interstitial site-selective nitrogen doping in TiO_2 nanostructures, J. Phys. Chem. C 119 (2015) 7452.
[20] D. Lin, C. Guo-xi, M. Ying, J. Xiao-lin, Y. Guo-tian, G. Shao-kang, Enhanced photocatalytic degradation properties of nitrogen-doped titania nanotube arrays, Trans. Nonferrous Metals Soc. China 19 (2009) 1583.
[21] N.C. Saha, H.G. Tompkins, Titanium nitride oxidation chemistry: an x-ray photoelectron spectroscopy study, J. Appl. Phys. 72 (1992) 3072.
[22] E. Galvanetto, F.P. Galliano, F. Borgioli, U. Bardi, A. Lavacchi, XRD and XPS study on reactive plasma sprayed titanium–titanium nitride coatings, Thin Solid Films 384 (2001) 223–229.
[23] A. Brudnik, M. Bucko, M. Radecka, A. Trenczek-Zajac, K. Zakrzewska, Microstructure and optical properties of photoactive TiO_2:N thin films, Vacuum 82 (2008) 936–941.